ELSEVIER

Journal of Nuclear Materials 305 (2002) 159–168

journal of nuclear materials

www.elsevier.com/locate/jnucmat

Densification behaviour of UO_2 in six different atmospheres

T.R.G. Kutty [a,*], P.V. Hegde [a], K.B. Khan [a], U. Basak [a], S.N. Pillai [a], A.K. Sengupta [a], G.C. Jain [a], S. Majumdar [a], H.S. Kamath [b], D.S.C. Purushotham [b]

[a] *Radiometallurgy Division, Bhabha Atomic Research Centre, Trombay, Mumbai 400 085, India*
[b] *Nuclear Fuels Group, Bhabha Atomic Research Centre, Trombay, Mumbai 400 085, India*

Received 8 January 2002; accepted 9 July 2002

Abstract

The shrinkage behaviour of UO_2 has been studied using a dilatometer in various atmospheres of Ar, Ar–8%H_2, vacuum, CO_2, commercial N_2 and $N_2 + 1000$ ppm of O_2. The onset of shrinkage occurs at around 300–400 °C lower in oxidizing atmospheres such as CO_2, commercial N_2 and $N_2 + 1000$ ppm O_2 compared to that in reducing or inert atmospheres. Shrinkage behaviour of UO_2 is almost identical in Ar, Ar–8%H_2 and vacuum. The shrinkage in $N_2 + 1000$ ppm O_2 begins at a lower temperature than that in the commercial N_2. The mechanism of sintering in the reducing, inert and vacuum atmospheres is explained by diffusion of uranium vacancies and that in the oxidizing atmospheres by cluster formation.

PACS: 81.20.Ev; 61.72.−y; 66.30.Fq

1. Introduction

UO_2 has been almost exclusively used as a fuel in commercial light and heavy water thermal reactors. The main advantages in the use of UO_2 are its high melting point, good dimensional and radiation stability and its excellent chemical compatibility with the other reactor components. The main disadvantages are, however, its low thermal conductivity and low fissile atom density which leads to give high centerline temperature and large volume cores respectively. In a stable fluorite structure, stoichiometric uranium dioxide crystallizes. It has a melting point of 2880 °C and exhibits a wide range of non-stoichiometry at elevated temperatures. This range extends from $UO_{1.65}$ to $UO_{2.25}$ at 2500 °C [1,2]. The hypostoichiometric UO_{2-x} exists only at high temperatures, whereas hyperstoichiometric UO_{2+x} exists even at low temperatures. A typical feature of the fluorite structure is the large $(1/2, 1/2, 1/2)$ interstitial holes in which the interstitial ions can easily be accommodated [3]. Thus, a large amount of interstitial oxygen can be dissolved causing to form extensive anion excess UO_{2+x}. The charge compensation for the excess of oxygen in UO_{2+x} is achieved by oxidizing U^{4+} to U^{5+} [4]. In this fluorite structure, uranium mobility is many orders of magnitude smaller than oxygen mobility, so that the rate determining step for the diffusion controlled processes such as sintering, grain growth, creep etc. is comprised of uranium diffusion. The ratio of oxygen diffusion coefficent and uranium diffusion coefficient, D^O/D^U, is reported to be greater than 10^5 at 1400 °C, suggesting that the uranium ion mobility is much smaller than the oxygen mobility. In fact, D^U increases in proportion to x^2 by about 5 orders of magnitude between UO_2 and $UO_{2.2}$ at 1400–1600 °C [5–7].

Uranium oxide fuel pellets for light and heavy water reactors are usually fabricated with an O/U ratio of around 2.00 in order to have better thermal properties and to achieve better compatibility between fuel, clad

* Corresponding author. Tel.: +91-22 559 2466/0663; fax: +91-22 550 5151.
E-mail address: tkutty@magnum.barc.ernet.in (T.R.G. Kutty).

0022-3115/02/$ - see front matter
PII: S0022-3115(02)00934-0

and coolant [1]. Large scale production of these pellets is carried out by powder metallurgical processes involving milling, pre-compaction and granulation followed by cold compaction and high temperature sintering in reducing atmosphere at around 1650 °C. For nuclear ceramics such as UO_2, it is reported that the diffusion rate is slow under reducing condition and is fast under oxidising condition [6]. For instance, if $UO_{2.1}$ is used rather than UO_2, D^U increases by a factor of 10^4 [7]. A change in the sintering atmosphere from reducing to controlled oxidizing conditions is therefore very much advantageous to increase the interdiffusion rates [8]. Uranium diffusion increases drastically in hyperstoichiometric oxide because of large increase in uranium vacancy concentration [1]. Short time sintering at low temperature ($\leqslant 1300$ °C) has been developed to take advantage of the enhanced uranium diffusion in hyperstoichiometric uranium oxides [1]. Sintering under oxidizing conditions with the associated fast diffusion proceeds in a short time at 1300 °C more rapidly than in a longer time at 1650 °C in reducing atmospheres. This process results in large scale savings in energy, time and capital investment [7]. However, there is a requirement for a subsequent reduction step to achieve the necessary O/U ratio, which would partially offset the above-mentioned advantages. Since diffusion is largely dependent on oxygen potential of the sintering atmosphere, it will be worthwhile to determine the effects of a wide variety of atmospheres such as inert (Ar), reducing (Ar–8%H_2), vacuum and oxidising (CO_2, commercial N_2 and $N_2 + 1000$ ppm O_2) atmospheres on the sintering behaviour of UO_2 using a dilatometer. So far, studies have not been reported on the above mentioned composition in such a wide range of atmospheres. Hence, it is felt that the results of this study would be very useful to the manufacturers of such fuels.

2. Experimental

2.1. Fabrication of green pellet

The green pellets for this study were prepared by the conventional powder metallurgy technique which consists of the following steps:

- milling uranium oxide powder in a planetary ball mill for 4 h using tungsten carbide ball,
- precompaction at around 150 MPa,
- granulating the conditioned powders,
- cold pressing of the granulated powders at around 300 MPa into green compact.

To facilitate compaction and to impart handling strength to the green pellets, 1 wt% zinc behenate was added as lubricant/binder during the last hour of milling. The characteristics of the UO_2 powder used in this study are given in Table 1.

Table 1
Characteristics of UO_2 powder

Property	Value
Oxygen to metal ratio	2.15
Apparent density (g/cm^3)	1.5
Total impurities (ppm)	<800
TD (g/cm^3)	10.96
Specific surface area, S (m^2/g)	3.0

2.2. Dilatometry

The details of the pellet used for the dilatometric studies are as given below:

- length, 7 mm;
- diameter, 4.6 mm;
- green density, $52 \pm 1\%$ of theoretical density (TD).

The shrinkage of the UO_2 pellets in the various atmospheres was measured in axial direction using a push rod type dilatometer (Netzsch, model 402 E/7). The sample supporter, measuring unit and displaceable furnace of the dilatometer were mounted horizontally. The length change measurements were made by a linear voltage differential transformer (LVDT), which was maintained at a constant temperature by means of water circulation from a constant temperature bath. The accuracy of the measurement of change in length was within ± 0.1 μm. The temperature was measured using a calibrated thermocouple which is placed directly above the sample. The dilatometry was carried out under the following condition:

- force on the sample, 0.2 N;
- gas flow, 18 l/h;
- heating rate, 6 °C/min.

The sintering in vacuum was carried out in a vacuum level better than 1 Pa. For $N_2 + 1000$ ppm O_2 atmosphere, 0.5 vol.% of dry air was mixed with pure N_2 gas using a gas mixer before admitting the gas into the dilatometer. The impurity contents of the cover gases used in this study are given in Table 2.

The heating rate used for the above studies was 6 °C/min. Length measurements were made in situ under dynamic condition. As the sample is heated, its temperature and length values are measured continuously with the help of a thermocouple and LVDT, respectively. The selection of the temperature programme was made by a computer via data acquisition system. The expansion of the system was corrected by taking a run

Table 2
Impurity contents of different sintering atmospheres

Sintering atmosphere	O_2 (ppm)	Moisture (ppm)	CO_2 (ppm)	CO (ppm)	N_2 (ppm)	Oxides of N_2 (ppm)	Hydrocarbon (ppm)
Ar	4	4	1	1	10	1	1.5
Ar + 8%H_2	4	4	1	1	10	1	2
CO_2	300–400	10	–	5	50	15	2
Commercial N_2	400–500	10	50	5	–	–	5
N_2 + 1000 ppm O_2	1000	5	1	1	–	–	3

under identical condition using a standard sample (POCO graphite, NIST).

2.3. Characterization

The uranium oxide pellets sintered in different atmospheres were characterized in terms of their density, oxygen to uranium ratio (O/U) and phase content. The O/U ratio was measured thermogravimetrically and the density was determined using immersion technique. Table 3 gives the typical values of O/U and their density. For metallography, the sintered pellet was mounted in bakelite and ground using successive grades of emery paper. The final polishing was done using diamond paste. The typical impurity contents in a sintered pellet are shown in Table 4.

Table 3
Density and O/U ratio of UO_2 pellets after sintering

Sintering atmosphere	Density (%TD)	O/U ratio
Ar	95	2.00
Ar–8%H_2	95	2.00
Vacuum	65	2.00
CO_2	90	2.10
Commercial N_2	90	2.05
N_2 + 1000 ppm O_2	88	2.07

Table 4
Metallic impurities in UO_2 pellet

Element	Impurity (ppm)
Na	<50
Ca	<120
Al	<10
Mg	<25
Si	<100
Fe	<150
Cr	<70
Co	<5
Ni	<60
Mo	<5
W	<50
B	<0.18

3. Results

Fig. 1 shows the dl/l_0 versus temperature plot of UO_2 under various atmospheres. The corresponding shrinkage rates $d(dl/l_0)/dt$ of the above pellet are shown in Fig. 2. It can be seen from Fig. 1 that the onset of shrinkage occurs at around 700 °C in CO_2. On the other hand, it begins between 1100 and 1150 °C in Ar, Ar–8%H_2 and vacuum. The commercial N_2 atmosphere behaves almost like CO_2 except that the shrinkage occurs at a slightly higher temperature (850 °C). In N_2 + 1000 ppm O_2, the onset of shrinkage starts at a lower temperature (700 °C) than that observed for the commercial N_2.

The dilatometric curve of Fig 1 was replotted as percentage of theoretical density (%TD) versus temperature (Fig. 3). The dl/l_0 values were converted into %TD (see Appendix A) using the following relation:

$$\rho = [1/(1 - dl/l_0)]^3 \rho_0, \quad (1)$$

where ρ and ρ_0 are the density of the sintered and green pellets respectively. At the highest temperature of 1650 °C, a density of around 95% of TD was obtained in Ar

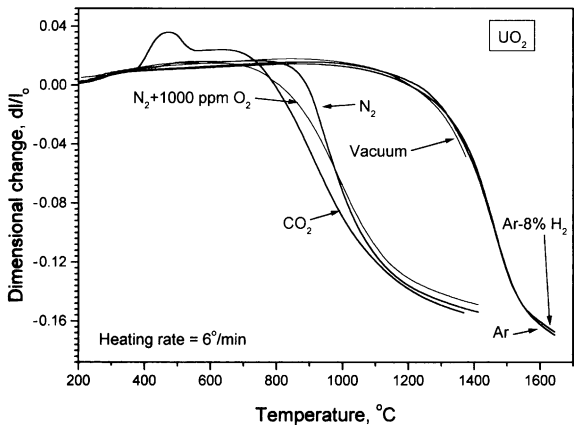

Fig. 1. Shrinkage curves for UO_2 pellets in Ar–8%H_2, Ar, vacuum, CO_2, commercial N_2 and N_2 + 1000 ppm O_2 atmospheres. The dl/l_0 values are plotted against temperature, where l_0 is the initial length.

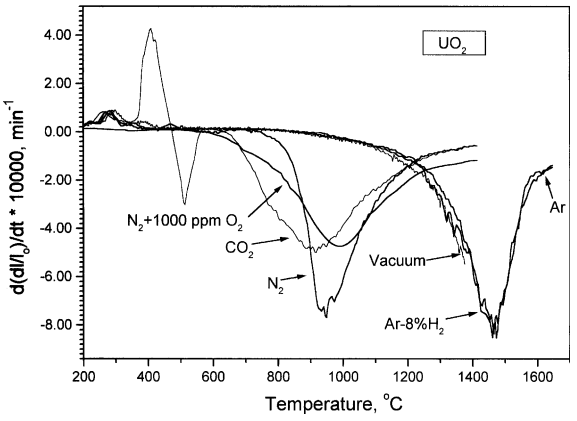

Fig. 2. Shrinkage rate $d(dl/l_0)/dt$ of UO_2 pellet in Ar–8%H_2, Ar, vacuum, CO_2, commercial N_2 and $N_2 + 1000$ ppm O_2 atmospheres plotted against temperature.

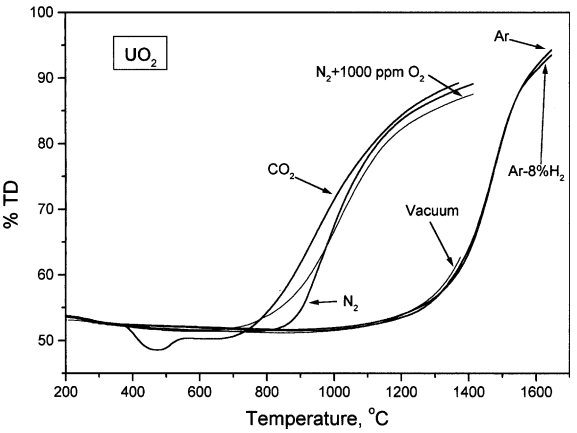

Fig. 3. Shrinkage curves of Fig. 1 is replotted as percent of theoretical density (%TD) versus temperature for UO_2 pellet for Ar–8%H_2, Ar, vacuum, CO_2, commercial N_2 and $N_2 + 1000$ ppm O_2 atmospheres. The values of dl/l_0 are converted into %TD as described in Appendix A.

and Ar–8%H_2. But in the oxidizing atmospheres even at 1350 °C, a density of around 90% of TD has been obtained. The sintering in vacuum has been carried out only up to 1400 °C which resulted in a very low density of only around 65% of TD.

A prominent peak was observed in the shrinkage curve between 350 and 500 °C in CO_2 atmosphere. This peak was absent for all other atmospheres. Another interesting phenomenon observed is that, for UO_2, the shrinkage behaviour in Ar, Ar–8%H_2 and vacuum is almost identical at all temperatures. From the shrinkage rate curves, it was observed that the maximum shrinkage rate occurs for N_2 atmosphere. The significant observations are summarized below:

1. Densification behaviour of UO_2 was found to be similar in Ar, Ar–8%H_2 and vacuum atmospheres.
2. The onset of sintering commences at a temperature which is about 300–400 °C lower in oxidizing atmosphere than that in the reducing and inert atmospheres.
3. The sintering commences at a slightly higher temperature for commercial N_2 atmosphere in comparison with CO_2.
4. The sintering behaviour in $N_2 + 1000$ ppm O_2 is almost similar to that in commercial N_2 except that the sintering commences at a temperature which is about 200 °C lower.
5. An expansion was noticed in the shrinkage curve of CO_2 in the temperature range of 350–500 °C.

4. Discussion

From the above results, it is clear that the onset of densification occurs above 1100–1150 °C for Ar, Ar–8%H_2 and vacuum. The sintering in oxidizing atmospheres commences about 300–400 °C lower than that in reducing and inert atmospheres. Sintering under oxidizing condition yields a density of 90%TD at around 1350 °C, which otherwise requires a temperature of 1600 °C for the reducing and inert atmospheres. At 1100 °C, the shrinkage does not occur in Ar–8%H_2. On the other hand, the shrinkage was quite appreciable in oxidizing medium (13% in CO_2) at the above mentioned temperature (see Fig. 1). These results are very important for the large scale fabrication of UO_2 sintered pellets since a change from the conventional reducing atmospheres to controlled oxidizing atmosphere results in huge savings in time and energy.

Sinterability of UO_2 compacts has been found to depend upon the following factors, namely [9–12]

1. sintering temperature,
2. sintering atmosphere,
3. characteristics of the starting UO_2 powders,
4. sintering time.

The sintering is caused by heat treatment of porous specimen without or with the application of external pressure, in which some properties of the pellet are changed with the reduction of the Gibbs free energy to those of the pore-free system [2]. The sintering process is usually divided into three stages in which different mechanisms may be operative [2,13–24]. They are

- Initial stage sintering, where the neck forms and grows between individual particles.
- Intermediate stage sintering, where the neck growth results in a body with continuous network of tubular pores.

- Final stage of sintering, where the pore shrinkage occurs, and most probably the pore becomes closed.

The sintering process is diffusion controlled one whose rate is controlled by the slower moving metal atoms. The point defect model has been used to explain many observed features of diffusion in non-stoichiometric fluorite type oxide fuels [1].

4.1. Point defect model

The point defect model attributes the observed changes in metal atom diffusion coefficient solely to the change in the point defect concentration brought about by the deviation of x from the stoichiometry while varying the oxygen potential. The point defect model was first developed by Matzke [25] and Lidiard [26]. Deviations from stoichiometry produce point defects, most likely oxygen vacancies or metal interstitials in hypostoichiometric compounds and oxygen interstitials or metal vacancies in hyperstoichiometric compounds. The point defects are also created thermally in these materials, provided the temperature is high enough. These defects can exist as single, isolated point defects at low concentration. At higher concentrations, the defects will aggregate into clusters, will become ordered or will be eliminated by the formation of two- or three-dimensional defects such as dislocation loops, shear planes, voids etc. [27–29].

A relation has been derived for the temperature dependence of the concentration of vacancies and interstitials in both the oxygen and metal sublattice by solving the anion Frenkel, Schottky and cation Frenkel defects (see Table 5). The uranium vacancy and uranium interstitial concentrations are calculated using the relations given in Table 5 for stoichiometric and non-stoichiometric compositions. The concentrations of uranium vacancies are plotted against O/U ratio for various temperatures in Fig. 4. Similarly, Fig. 5 shows the uranium interstitial concentrations at various temperatures plotted against O/U ratio. From Fig. 4, it is clear that there is a drastic change in the uranium vacancy concentration on varying O/U around the stoichiometric composition.

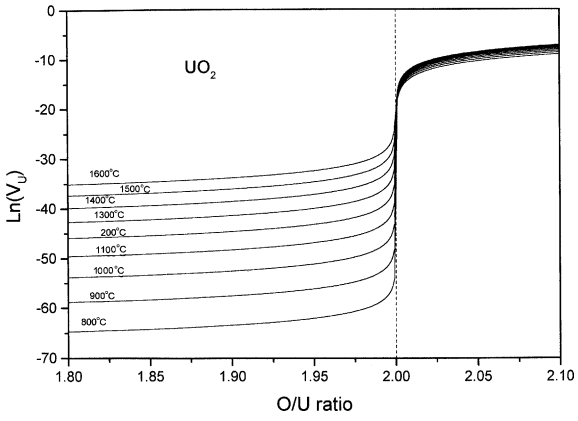

Fig. 4. Concentration of uranium metal vacancies as plotted against O/U ratio at various temperatures. The concentration of uranium vacancies are calculated using the point defect model described in Table 5.

4.2. Previous work on UO_2

Extensive researches on the sintering behaviour of UO_2 have been reported. Lay and Carter [30] have studied the role of O/U ratio on sintering of UO_2 and reported that the uranium diffusion coefficient at the initial stages of sintering is dependent up on the O/U ratio. They have shown that the uranium diffusion coefficient of UO_2 in CO_2/CO atmosphere having an O/U ratio of 2.02 is 10^8 times greater than that in H_2 atmosphere having an O/U ratio of 2.00. They have also

Table 5
Standard point defect model of fluorite type oxides $UO_{2\pm x}$ and energies for different defect processes [1,25–27]

Defect concentrations	Stoichiometric $UO_{2.00}$	$[V_U] = 2\exp[-(\Delta G_s - \Delta G_{FO})/kT]$ $[U_i] = 0.5\exp[-(\Delta G_{FU} + \Delta G_{FO} - \Delta G_s)/kT]$
	Hyperstoichiometric UO_{2+x}	$[V_U] = x^2\exp[-(\Delta G_s - 2\Delta G_{FO})/kT]$ $[U_i] = (1/x^2)\exp[-(\Delta G_{FU} + 2\Delta G_{FO} - \Delta G_s)/kT]$
	Hypostoichiometric UO_{2-x}	$[V_U] = (4/x^2)\exp[-\Delta G_s/kT]$ $[U_i] = (x^2/4)\exp[-(\Delta G_{FU} - \Delta G_s)/kT]$
Formation energies (eV)	Oxygen Frenkel pair, ΔG_{FO}	3.0
	Metal Frenkel pair, ΔG_{FU}	7.0
	Schottky trio, ΔG_S	6.4
Migration energies (eV)	Oxygen vacancy, ΔH^m_{VO}	0.53
	Oxygen interstitial, ΔH^m_{Oi}	0.64
	Metal vacancy, ΔH^m_{VU}	6.0
	Metal interstitial, ΔH^m_{Ui}	8.76

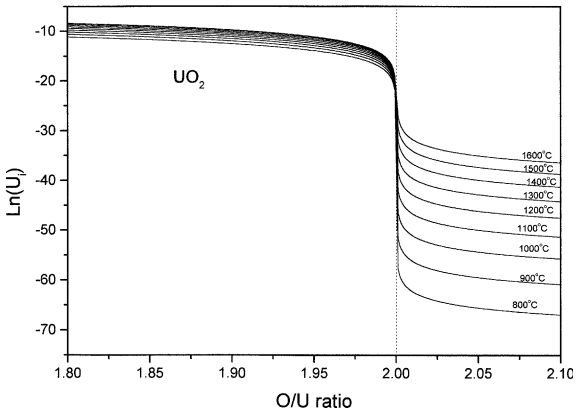

Fig. 5. Concentration of uranium interstitials as plotted against O/U ratio at various temperatures.

shown that the sintering rate is independent of the initial O/U ratio of the starting powder. The effect of non-stoichiometry has also been studied by Murray et al. [31] who found large differences in the sintering behaviour for the different O/U ratios. They attributed this to the formation of U_4O_9. Webster [32] reported enhanced sintering in steam and in CO_2. Williams et al. [33] studied the effect of various atmospheres on the sintering behaviour of UO_2. Bailey [34] suggested the advantages of steam sintering while Amato [35] employed CO_2 sintering, followed by H_2 reduction. Langrod [36] used mixtures of UO_2 and U_3O_8 as a starting material and used N_2 as the sintering gas followed by H_2 reduction.

Assmann et al. [37,38] studied the microstructure of UO_2 on oxidative sintering. They have found that the use of CO_2 as sintering atmosphere is very favourable for solarization, which in turn helps in achieving very low ratio of open/closed porosity with very high sphericity. They suggested a controlled path sintering which is based on the control of U–O phases at the sintering stage where pronounced grain growth takes place. The stoichiometry of UO_{2+x}/U_4O_{9-y} is controlled by the oxygen activity of the sintering gas. In another study, Matzke [39] had carried out annealing experiment in various atmospheres such as vacuum, dry H_2, Ar, N_2 and N_2/H_2 mixtures. He reported that the activation enthalpy for UO_{2+x} is lower by ΔG_{FO} compared to the activation enthalpy for UO_2 where ΔG_{FO} is the free energy of the oxygen Frenkel defect formation.

Langrod [36] and Fuhrman et al. [40] showed that the UO_2 pellets produced by a two stage low temperature sintering process could be sintered to at least 95%TD at 1200 °C in N_2 atmosphere. They showed that an O/U ratio of 2.25 is required to achieve such a high density. In order to achieve the final O/U ratio of 2.00, hydrogen soaking for 1 h was required at that temperature. Korean researchers [41,42] have shown that UO_2 pellets could be easily sintered using a two stage process which consists of heating in an atmosphere of CO_2/CO gas mixtures and then changing the cover gas to H_2 at a lower temperature. Ganguly and Basak [43] reported the fabrication of high density UO_2 pellets at 1300 °C in CO_2 followed by a reductive treatment. These pellets have been irradiated in PHWR and are reported to show good performance. Harada [44] suggested a three stage sintering process for the fabrication of UO_2 pellets. His three stage process consists of sintering in reducing–oxidizing–reducing atmospheres at low temperatures between 1200 and 1500 °C. Since the pellets are reduced during the heating up of first reducing cycle, the sinterability is independent of the initial O/U ratio. After attaining the sintering temperature, the atmosphere was changed from reducing to oxidizing one where the oxygen partial pressure is adjusted to the boundary between single phase UO_{2+x} and UO_{2+x}–U_3O_{8-z}. The enhanced oxygen partial pressure helps in attaining high density and larger grain size. In the third stage, the O/U ratio was brought down around 2.00 by subsequent reduction in N_2/H_2 mixture. The dimensional stability of the three stage process during the resintering test was found to be superior than that of the two stage sintering. Chevrel et al. [45] indicated that the composition of $UO_{2.25}$ appeared to be the most appropriate for the low temperature sintering. An O/U ratio of 2.25 was obtained by the addition of U_3O_8 powder to UO_2.

With the above background in mind, we will discuss the effect of various atmospheres on the shrinkage behaviour of the UO_2. Possible mechanisms for the densification in each of the atmospheres have been suggested.

4.3. Ar–8%H_2

As mentioned earlier, in reactor technology, stoichiometric UO_2 is needed and therefore sintering is carried out in reducing atmosphere. This requires high temperature of approximately 1700 °C. During the fabrication of oxide fuel under reducing condition, the oxygen potential is not generally controlled, which is generally in the range of −30 to −120 kcal/mol, typical for dry H_2 [1,46,47]. Since the H_2O/H_2 ratio in the Ar–8%H_2 sintering gas used in this study is less than 10^{-4}, a highly reducing environment is ensured inside the sintering furnace [48]. The O/U ratio of the pellet sintered in Ar–8%H_2 is 2.00 as shown in Table 3. This means that it has a low defect concentration.

From Figs. 4 and 5, it is evident that the concentration of uranium vacancies and uranium interstitials are considerably less near the stoichiometric composition at all temperatures. Since the concentration of defects is very low in a pellet sintered in Ar–8%H_2, the driving force for the sintering is also small. Hence it requires a high temperature of approximately 1700 °C to attain a density of 95% TD and above. From Figs. 4 and 5, it is

also clear that at the stoichiometric composition, the concentration of uranium vacancies is higher than that of uranium interstitials. Hence, the vacancy mechanism seems to hold for above composition when sintered in Ar–8%H_2.

4.4. Ar

The densification behaviour of UO_2 in Ar has been found to be similar to that in Ar–8%H_2. The samples sintered in Ar and Ar–8%H_2 have almost identical O/U (see Table 3). This means that UO_{2+x} loses oxygen in Ar at high temperatures and becomes stoichiometric, resulting in a similar defect concentration as that found in the case of Ar–8%H_2, which is very low. Therefore, sintering commences only at a higher temperature of ~1100 °C and above. The sintering mechanism based on uranium vacancies has been suggested for the densification behaviour in Ar. The microstructure of the pellet sintered in Ar was found to be similar to that in Ar–8%H_2. The grain size was found to be uniform with an average grain size of around 15 μm.

A difference was noted in the shrinkage rate curves of Ar and Ar–8%H_2 shown in Fig. 2. The shrinkage rate curves for Ar was found to be smooth while that for Ar–8%H_2 showed many oscillations especially in the temperature range of 1100–1600 °C. This may be due to some micromechanisms occurring in the pellet during the sintering. Similar observations were noted for PuO_2 when sintered in Ar–8%H_2 [49].

4.5. Vacuum

The densification studies in vacuum have been carried out only up to 1400 °C. The vacuum used for this experiment was neither too high nor very coarse. A mechanical pump was used for evacuation and a vacuum level of 1 Pa was maintained during the experiment. The shrinkage curves for vacuum exactly coincides with that for Ar and Ar–8%H_2. Since the sintering was carried out only up to 1400 °C in vacuum, a final density of around 65% was only obtained for this pellet (see Fig. 3). Kamath et al. [50] have conducted studies on UO_2 in coarse vacuum of 10 Pa, and reported that such coarse vacuum helps in attaining high density at a low temperature of 1300 °C. They did not use any admixed binder in the powder but used only die wall lubrication during compaction. It is reported [50] that the binder leaves some residual carbon in the pellet even after its removal at low temperature of 300 °C. This residual carbon takes away oxygen from hyperstoichiometric oxide and thus reducing the O/U ratio which in turn adversely affects the sinterability. In large scale production of UO_2 pellets, a small quantity of binder/lubricant is generally added to facilitate automatic compaction of pellets. Keeping this in mind, the present study has been carried out with admixed binder/lubricant. Further studies are planned on the effect of binder and its optimum amount to be used in large scale production of UO_2 pellets.

The O/U ratio of the pellet, sintered in vacuum, has been found to be exactly 2.00 and therefore defect levels are low as mentioned earlier. The maximum temperature for the sintering was 1400 °C instead of 1650 °C used for Ar and Ar–8%H_2 atmospheres. These two factors, namely low temperature and the O/U value of 2, gave poor shrinkage behaviour.

4.6. CO_2

A sintered density of approximately 90%TD was obtained at a temperature as low as 1300 °C when the sintering atmosphere was CO_2. The O/U ratio of the pellet sintered in CO_2 is 2.10 which indicates that there are considerably higher concentrations of metal vacancies present in the system. Lay and Carter [30] have shown that uranium self-diffusion coefficient in UO_{2+x} is proportional to x^2. This is predominantly due to the increased concentration of uranium vacancies in UO_{2+x}. From Fig. 4, it can be seen that the metal vacancy concentration is very high for UO_2 when sintered in CO_2 atmosphere. But at such a high concentration, defects will aggregate into clusters [51–53].

Willis [54] has made detailed investigation of the defect structure of UO_{2+x} using Bragg neutron scattering technique. He found the evidence for two types of interstitials, one (O′) displaced from $(1/2, 1/2, 1/2)$ positions along $\langle 1\,1\,0\rangle$ axis and the other (O″) displaced along the $\langle 1\,1\,1\rangle$ axis. In addition a significant number of normal oxygen atoms are displaced, thus creating oxygen vacancies which are identical in number with either of the $\langle 1\,1\,0\rangle$ and $\langle 1\,1\,1\rangle$ interstitials. Willis proposed a defect cluster containing two O′ interstitials, two O″ interstitials and two normal oxygen vacancies which is commonly known as 2:2:2 or Willis cluster. A more careful study on uranium sublattice indicates that the uranium atoms are displaced by 0.25 Å from their normal positions. Hence, oxygen diffusion will be drastically modified by the vacancies and interstitials in UO_{2-x} and in UO_{2+x}. However, cation transport coefficient will also be modified by the coupling of the Schottky and Frenkel disorder reaction, the effect of which is to enhance cation vacancies in the UO_{2+x} and suppress them in UO_{2-x}. Therefore, the cluster mechanism is suggested to hold for the pellets sintered in CO_2.

During the sintering of UO_2, a prominent peak was observed in the shrinkage curve at around 350–500 °C (see Fig. 1). Kutty et al. [48] argued that this peak is due to the surface oxidation of UO_2. The surface layers of the UO_2 are oxidized to U_3O_7. The oxidation behaviour of UO_2 in various atmospheres has been studied by many authors [55–63]. Blackburn et al. [55] showed that

UO_2 is oxidized with immediate formation of a surface U_3O_7 phase, the process of which is controlled by the diffusion of the oxygen through the second phase. Gasic et al. [56] conducted differential thermal analysis of UO_2 oxidation and showed that the above process takes place in two stages. In the first stage UO_2 is oxidized to U_3O_7, which is followed by the conversion of U_3O_7 into U_3O_8. Olander [57] showed that the oxidation behaviour of UO_2 is very sensitive to H/O (hydrogen to oxygen atom) ratio of the atmosphere. Tempest et al. [58] evaluated the oxidation of UO_2 pellet in air at 230 and 270 °C. Their study also revealed that the first product of oxidation of UO_2 was always U_3O_7 which on very long time annealing in air converted to U_3O_8. To understand the oxidation behaviour of UO_2 in CO_2, a detailed thermal analysis was carried out.

For the analysis, UO_2 powder having an initial O/U ratio of 2.15 was heated in a thermobalance up to 600 °C in CO_2 atmosphere at a heating rate of 6 °C/min. The resultant thermogram is shown in Fig. 6. From the figure, it is evident that there are two regions of weight gain, the first one being in the temperature range of 150–250 °C and the second in the range of 350–500 °C. The gain in the first instance corresponds to the formation of U_4O_{9-y} and the second one corresponds to the formation of U_3O_7. The formation of U_3O_8 has been ruled out since it will result in a volume change of around 30%. Such drastic volume change will result in spallation and production of particulates which will cause the pellet to disintegrate. Since no powder or particulate formation had been noticed on the surface during sintering in CO_2 atmosphere, it can be said that the oxygen potential of the above atmosphere is not sufficient to cause UO_2 to oxidize to U_3O_8.

The UO_2 powder used for this study had an O/U ratio of 2.15 and hence the corresponding phases of the

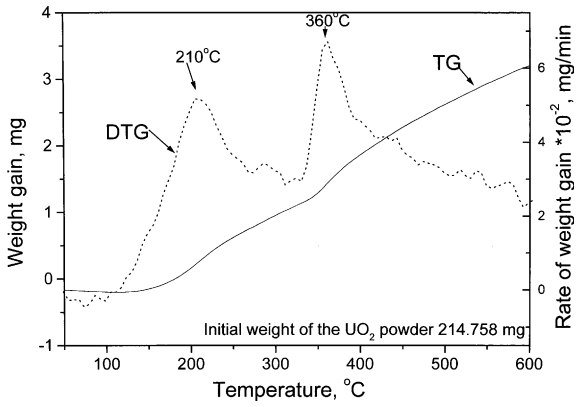

Fig. 6. Weight gain obtained in thermogravimetric studies against temperature for UO_2 powder heated in CO_2 atmosphere. The initial O/U ratio of UO_2 powder was 2.15 and its initial weight was 214.758 mg.

powder at room temperature should be $UO_2 + U_4O_{9-y}$ [5]. As the temperature increases, the surface oxidation of UO_2 takes place as explained above. The formation of U_3O_7 by the incorporation of extra oxygen atoms resulted in intergranular and transgranular cracking of the surface but did not cause gross disruption of the surface or spallation [58–60]. This formation reaction caused the expansion which is manifested in the shrinkage curve at around 350 °C (Fig. 1). Through the cracks, CO_2 gas penetrates and oxidizes the inner layers. But the inner layers are not oxidized to U_3O_7 instead some of UO_{2+x} has taken up more oxygen in the lattice forming UO_{2+y} ($y > x$). This means that the some of U^{4+} ions are converted to U^{5+} or U^{6+} ions [61–63]. Since ionic radii of U^{5+} (0.87 Å) and U^{6+} (0.83 Å) are smaller than that of U^{4+} (0.97 Å), the lattice shrinks. Thus the expansion in the shrinkage curve is due to the formation of U_3O_7 on the outer surface and consequent shrinkage is due to the oxidation of the inner layers.

4.7. Commercial N_2

The shrinkage behaviour of UO_{2+x} in commercial N_2 is almost identical to that in CO_2. Since the commercial N_2 contains about 500 ppm of oxygen, it has enough oxygen to oxidize UO_2 to UO_{2+x}. The O/U ratio of the pellet sintered in commercial N_2 is about 2.05. Obviously the fast diffusion of uranium in UO_{2+x} is due to the increased metal vacancy concentration. The maximum shrinkage rate was found to be around 40 μm/min, which occurred at 925 °C. The maximum shrinkage rate for CO_2 was found to be lower than that for commercial N_2 but was observed at a lower temperature of around 900 °C. Another interesting feature observed from the shrinkage rate curves of UO_{2+x} in commercial N_2 and CO_2 is the shape of the curve. The shrinkage rate curves for CO_2 was found to be wide and shallow while that for commercial N_2 was found to be narrow and deep (see Fig. 2). Since the pellet has deviated from the stoichiometry considerably, the mechanism suggested for the sintering is the cluster formation.

4.8. N_2 + 1000 ppm of O_2

In commercial nitrogen atmosphere, sintering can be carried out at a temperature as low as 1300 °C. Since the diffusion is largely dependent on oxygen potential of the sintering atmosphere, an attempt was made to sinter UO_2 in an atmosphere of N_2 containing 1000 ppm of O_2. The shrinkage curve for the above mentioned atmosphere was found to be similar to the one that found for commercial N_2 except that the shrinkage starts at much lower temperature than that observed for the commercial N_2. This shows that mixing of air with commercial N_2 is one of the cheaper way of attaining very high density UO_2 pellets at a relatively lower temperature.

The O/U ratio of the pellet (2.07) was found to be higher than that obtained in commercial N_2 but was less than that in CO_2 atmosphere. Again, the high concentration of uranium vacancies present in these pellets affected to give fast shrinkage. The mechanism for the densification is the same as that proposed for CO_2 and commercial N_2.

Microstructure of the pellets showed duplex grain structure. The average grain size was found to be 8 μm. There were pockets of fine grains of 2–3 μm at many places. The pellets sintered in CO_2 and commercial N_2 showed an identical microstructure.

5. Conclusions

The sintering behaviour of UO_2 was studied in a wide range of atmospheres such as inert, reducing, vacuum and oxidising atmospheres. The following conclusions were drawn:

1. Shrinkage begins at a much lower temperature in oxidising atmosphere such as CO_2, commercial N_2 and $N_2 + 1000$ ppm O_2. The shrinkage begins around 300–400 °C lower compared to that in reducing or inert atmospheres.
2. Shrinkage behaviour of UO_2 is almost identical in Ar, Ar–8%H_2 and vacuum.
3. The shrinkage behaviour in $N_2 + 1000$ ppm O_2 begins at lower temperature than that in the commercial N_2.
4. The shrinkage rate was found to be maximum in commercial nitrogen atmosphere for UO_2.
5. The mechanism of sintering for the reducing, inert and vacuum atmospheres is due to the diffusion of uranium vacancies and that for the oxidizing atmospheres are due to the cluster formation.

Acknowledgements

The authors wish to record their sincere thanks to Dr S.K. Mukherjee for useful discussion. They also thank Messers T. Jarvis, V.D. Alur, K. Ravi, P. Sankaran Kutty and G.P. Mishra for their support during the course of this work.

Appendix A. Conversion of dl/l_0 values to percent of theoretical density

Let the initial length and radius of the green pellet be l_0 and r_0 respectively and its green density be ρ_0 %TD. At certain elevated temperature, T, its length and radius be l_1 and r_1 respectively and hence shrinkage is dl/l_0. Therefore,

$$l_1 = (1 + \Delta l/l_0)l_0 \quad \text{and} \quad r_1 = (1 + \Delta l/l_0)r_0. \tag{A.1}$$

$$\text{Initial volume, } V_0 = \pi r_0^2 l_0. \tag{A.2}$$

$$\begin{aligned}\text{Sintered volume, } V_1 &= \pi r_1^2 l_1 \\ &= \pi(1 + \Delta l/l_0)^2 r_0^2 (1 + \Delta l/l_0) l_0 \\ &= \pi r_0^2 l_0 (1 + \Delta l/l_0)^3 \\ &= V_0(1 + \Delta l/l_0)^3. \end{aligned} \tag{A.3}$$

The change in density,

$$\Delta\rho = \rho_1 - \rho_0 = (M/V_1) - (M/V_0) \tag{A.4}$$

$$= M/V_0\{1/(1 + \Delta l/l_0)^3 - 1\} \tag{A.5}$$

$$= \rho_0\{1/(1 + \Delta l/l_0)^3 - 1\}. \tag{A.6}$$

Hence

$$\Delta\rho/\rho_0 = \{1/(1 + \Delta l/l_0)^3 - 1\}. \tag{A.7}$$

At temperature, T, density of the pellet in terms of %TD

$$= (1 + \Delta\rho/\rho_0) \times \%\text{TD of green pellet}$$

$$= \{1/(1 + \Delta l/l_0)^3\} \times \rho_0\%\text{TD}. \tag{A.8}$$

Thus dl/l_0 versus T curve can be converted into %TD versus T curve.

References

[1] Hj. Matzke, in: T. Sorensen (Ed.), Non-stoichiometric Oxides, Academic, New York, 1981, p. 156.
[2] D.R. Olander, Fundamental Aspects of Nuclear Reactor Fuel Elements, TID-26711-P1, US Department of Energy, 1976, p. 145.
[3] R.W. Cahn, P. Haasen, E.J. Krammer, B.R.T. Frost, in: Materials Science and Technology, A Comprehensive Review, vol. 10A, VCH, New York, 1994, p. 114.
[4] C.R.A. Catlow, J. Chem. Soc. Faraday Trans. 83 (1987) 1065.
[5] J. Belle, J. Nucl. Mater. 30 (1969) 3.
[6] C.R.A. Catlow, A.B. Lidiard, in: Proceedings of Symposium on Thermodynamics of Reactor Materials, IAEA, Vienna, vol. II, 1974, p. 27.
[7] Hj. Matzke, J. Chem. Soc. Faraday Trans. 86 (1990) 1243.
[8] R. Thiessen, D. Vollath, in: Plutonium as a Reactor Fuel, IAEA, Vienna, 1967, p. 253.
[9] P. Balakrishnan, B.N. Murthy, K.P. Chakraborthy, R.N. Jayaraj, C. Ganguly, J. Nucl. Mater. 297 (2001) 35.
[10] J.L. Wolfrey, J. Am. Ceram. Soc. 55 (1972) 383.
[11] M. Peehs, H. Assmann, R. Manzel, V. Mathieu, in: Proceedings of International Symposium on Improvements in Water Reactor Fuel Technology and Utilization, Stockholm, Sweden, 25–19 September 1986, IAEA, Vienna, 1987, IAEA-SM-288/23.
[12] R. Manzel, W.O. Dorr, Ceram. Bull. 59 (6) (1980) 601, 616.

[13] F. Thummler, W. Thomma, Metall. Rev. 115 (1967) 69.
[14] R.L. Coble, J.E. Burke, in: J.E. Burke (Ed.), Progress in Ceramic Science, vol. 3, Pergamon, Oxford, 1963, p. 197.
[15] M. Mayo, Int. Mater. Rev. 41 (3) (1996) 85.
[16] H. Palmour, D.R. Johnson, in: G.C. Kuczynski, N.A. Hooton, C.F. Gibbs (Eds.), Sintering and Related Phenomena, Gordon and Breach, New York, 1967, p. 779.
[17] D.S. Perera, M.W.A. Stewart, Mater. Forum 20 (1996) 145.
[18] H. Kramer, J. Mater. Sci. Lett. 14 (1995) 778.
[19] D.L. Johnson, T.M. Clarke, Acta Metall. 12 (1964) 1173.
[20] R.L. Coble, J. Am. Ceram. Soc. 41 (1958) 55.
[21] D.L. Johnson, I.B. Cutler, J. Am. Ceram. Soc. 46 (1963) 541.
[22] W.D. Kingery, M. Berg, J. Appl. Phys. 26 (1955) 1205.
[23] L. Berrin, D.L. Johnson, in: G.C. Kuczynski, N.A. Hooton, C.F. Gibbs (Eds.), Sintering and Related Phenomena, Gordon and Breach, New York, 1967, p. 369.
[24] D.L. Johnson, J. Appl. Phys. 40 (1969) 192.
[25] Hj. Matzke, Atomic Energy Canada Ltd. Report AECL – 2585, 1966.
[26] A.B. Lidiard, J. Nucl. Mater. 19 (1966) 106.
[27] R.A. Jackson, C.A. Catlow, A.D. Murray, J. Chem. Soc. Faraday Trans. 83 (2) (1987) 1171.
[28] C.R.A. Catlow, in: T. Sorensen (Ed.), Non-Stoichiometric Oxides, Academic, New York, 1981, p. 61.
[29] G.E. Murch, C.A. Catlow, J. Chem. Soc. Faradays Trans. 83 (2) (1987) 1157.
[30] K.W. Lay, R.E. Carter, J. Nucl. Mater. 30 (1969) 74.
[31] P. Murray, S.F. Pugh, J. Williams, Fuels Elements Conference, AEC, Paris, 1957, p. 432.
[32] A.H. Webster, N.F.H. Bright, Department of Mines and Technical Surveys, Ottawa, Mines Branch Research Report, February 1958.
[33] J. Williams, E. Barnes, R. Scott, A. Hall, J. Nucl. Mater. 1 (1959) 28.
[34] W.E. Baily, J.C. Danko, H.M. Ferrari, R. Colombo, Am. Ceram. Soc. Bull. 41 (1962) 768.
[35] I. Amato, R.L. Colombo, A.M. Protti, Nucl. Sci. Eng. 16 (1963) 137.
[36] K. Langrod, Am. Ceram. Soc. Bull. 39 (7) (1960) 366.
[37] H. Assmann, W. Doerr, M. Peehs, J. Am. Ceram. Soc. 67 (9) (1984) 631.
[38] H. Assmann, W. Doerr, M. Peehs, J. Nucl. Mater. 140 (1986) 1.
[39] Hj. Matzke, J. Nucl. Mater. 114 (1983) 121.
[40] N. Fuhrman, L.D. Hower, B.R. Holden, J. Am. Ceram. Soc. 46 (3) (1963) 114.
[41] K.W. Song, D. Sohn, W.K. Choo, J. Nucl. Mater. 200 (1993) 41.
[42] K.W. Song, W.K. Choo, J. Nucl. Mater. 203 (1993) 122.
[43] C. Ganguly, U. Basak, J. Nucl. Mater. 178 (1991) 179.
[44] Y. Harada, J. Nucl. Mater. 245 (1997) 217.
[45] H. Chevrel, P. Dehaudt, B. Francois, J.F. Baumard, J. Nucl. Mater. 189 (1992) 175.
[46] Hj. Matzke, Philos. Mag. 64A (1991) 1181.
[47] D. Glasser-Leme, Hj. Matzke, Solid State Ion. 12 (1984) 217.
[48] T.R.G. Kutty, P.V. Hegde, K.B. Khan, S. Majumdar, D.S.C. Purushotham, J. Nucl. Mater. 281 (2000) 10.
[49] T.R.G. Kutty, K.B. Khan, P.V. Hegde, A.K. Sengupta, S. Majumdar, D.S.C. Purushotham, J. Nucl. Mater. 297 (2001) 120.
[50] H.S. Kamath, D.S.C. Purushotham, D.N. Sah, P.R. Roy, in: Proceedings of IAEA-SM on Improved Utilization of Water Reactor Fuels, Mol, Belgium, 7–11 May 1984, IAEA, Vienna, 1984.
[51] M. Coquerelle, Hj. Matzke, C.T. Walker, in: Proceedings of IAEA Technical Committee Meeting on Recycling of Plutonium and Uranium in Water Reactor Fuels, Cadarache, 13–16 November 1989, paper no. 23.
[52] M.H. Rand, T.L. Markin, Thermodynamics of Nuclear Materials, IAEA, Vienna, 1967, p. 637.
[53] Hj. Matzke, J. Chem. Soc. Faraday Trans. 83 (1987) 1121.
[54] B.T.M. Wills, Acta Crystallogr. 18 (1965) 75.
[55] P.E. Blackburn, J. Weissbart, E.A. Gulbransen, J. Phys. Chem. 62 (1958) 902.
[56] M.C. Gasic, S.B. Boskovic, V.D. Mikijelj, M.M. Ristic, in: M.M. Ristic (Ed.), Uranium Dioxide, Boris Kidric Institute of Nuclear Sciences, Belgrade, 1971, p. 1.
[57] D.R. Olander, Nucl. Technol. 74 (1986) 215.
[58] P.A. Tempest, P.M. Tucker, J.W. Tyler, J. Nucl. Mater. 151 (1988) 251.
[59] G.C. Allen, J.W. Tyler, J. Chem. Soc. Faraday Trans. 82 (1986) 1367.
[60] G.C. Allen, P.A. Tempest, J.W. Tyler, J. Chem. Soc. Faraday Trans. 83 (1987) 925.
[61] Thermodynamic and Transport Properties of Uranium Dioxide and Related Phases, Technical Reports Series no. 39, IAEA, Vienna, 1965, p. 51.
[62] W.I. Stuart, R.B. Adams, J. Nucl. Mater. 58 (1975) 201.
[63] K.T. Harrison, C. Padgett, K.T. Scott, J. Nucl. Mater. 23 (1967) 121.